High pressure-high temperature phase diagram of ammonia

Sandra Ninet, Frédéric Datchi

High pressure-high temperature phase diagram of ammonia

S. Ninet* and F. Datchi

Institut de Minéralogie et de Physique des Milieux Condensés,

Département Physique des Milieux Denses, CNRS UMR 7590,

Université Pierre et Marie Curie - Paris VI,

4 place Jussieu, 75252 Paris Cedex 05, France.

(Dated: January 7, 2008)

Abstract

The high pressure(P)-high temperature(T) phase diagram of solid ammonia has been investigated using diamond anvil cell and resistive heating techniques. The III-IV transition line has been determined up to 20 GPa and 500 K both on compression and decompression paths. No discontinuity is observed at the expected location for the III-IV-V triple point. The melting line has been determined by visual observations of the fluid-solid equilibrium up to 9 GPa and 900 K. The experimental data is well fitted by a Simon-Glatzel equation in the covered P-T range. These transition lines and their extrapolations are compared with reported *ab initio* calculations.

PACS numbers: 62.50.+p,64.70.Dv,64.70.K,61.50.-f,63.20.-e,64.60.-i

I. INTRODUCTION

Giant planets are mainly composed of simple molecular compounds such as H_2O, H_2, He, CH_4 and NH_3[1]. In particular, a layer of mixed ices (NH_3, H_2O, CH_4) has been proposed to exist in the interior of Uranus and Neptune. In this layer, extreme thermodynamic conditions are supposed (20<P<300 GPa and 2000<T<5000 K)[2] and the knowledge of the properties of these "hot" ices are crucial to a good examination of astrophysical data.

Experimental data under high P-T conditions are also very important to validate *ab initio* calculations[3,4] performed on NH_3 and H_2O. A very similar phase diagram has been predicted for these two compounds. In particular, a spectacular superionic phase is predicted at high pressures and temperatures[3]. In this phase, the molecular nature of these ices disappears and hydrogen atoms diffuse in all the N- or O- network. This prediction has stimulated many recent experimental works on the melting curve of water as the latter is expected to exhibit a clear kink at the onset of the transition. A change of slope in the melting curve of water ice has been reported in three different experimental studies, but its location substantially differ between them: 47 GPa and 1000 K in Ref. 5, 43 GPa and 1500 K in Ref. 6, and 35 GPa and 1040 K in Ref. 7. By contrast, no discontinuity has been observed in another melting study up to 50 GPa and 1100 K[8]. Theoretical predictions of the fluid-superionic solid transition pressure range between 30 and 75 GPa at 2000 K[3,4]. The exact location of the superionic phase is important for models of planetary interiors as it determines for example whether the Neptune and Uranus isentropes cross the superionic phase.

Unlike water, experimental data on ammonia under high static P-T conditions are very scarce. Experiments in a diamond anvil cell have been so far limited to 373 K[9]. Several shock-wave experiments[10,11,12,13,14] have reported equation of state and electrical conductivity data in the range ∼2-65 GPa, 1100-4600 K, but these are restricted to the fluid phase. New experiments are thus needed to bridge the present gap between static and dynamic investigations.

The presently accepted phase diagram of ammonia is shown in Fig. 1. Above 4 GPa, three different phases may be stabilized depending on the temperature. In increasing order of temperature, these are the ordered, orthorhombic phase IV, the plastic (orientationally disordered) cubic phase III, and the fluid. The IV-III and III-fluid transition lines have been determined up to 373 K[9,16,17]. Evidences for a solid phase transition in NH_3 at 14 GPa and

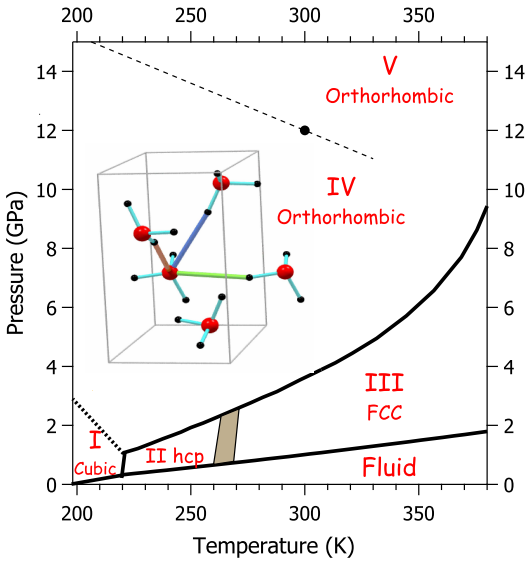

FIG. 1: (Color online) Phase diagram of ammonia (NH_3). The structure of phase IV as determined by Loveday *et al*[15] is depicted.

300 K to phase V were initially reported by Gauthier *et al.* using Raman[18] and Brillouin[19] spectroscopies. We recently confirmed this transition using single-crystal x-ray diffraction[20] and Raman spectroscopy[21], but unlike Gauthier *et al.*'s suggestion of a cubic structure for the high pressure phase, we found that the latter is isostructural to phase IV (space group $P2_12_12_1$). The transition was detected at 12 and 18 GPa for NH_3 and ND_3 respectively at room temperature.

In this paper, we report experimental measurements of the phase diagram of NH_3 in the range [1-20 GPa] and [300-900K]. The III-IV transition line has been determined up to 20 GPa and 500 K in order to detect the influence of the isostructural phase transition. The melting curve has been determined up to 9 GPa and 905 K. No evidence for the superionic phase has been observed in this P-T range.

II. EXPERIMENTAL METHODS

Samples of NH_3 were cryogenically loaded in membrane diamond anvil cells as described in Refs. [20,22]. A gold ring between the rhenium gasket and the sample was employed to prevent any possible chemical reaction between ammonia and rhenium at high temperature. Pressure was determined with the luminescence of SrB_4O_7:Sm^{2+} at high temperature[23,24].

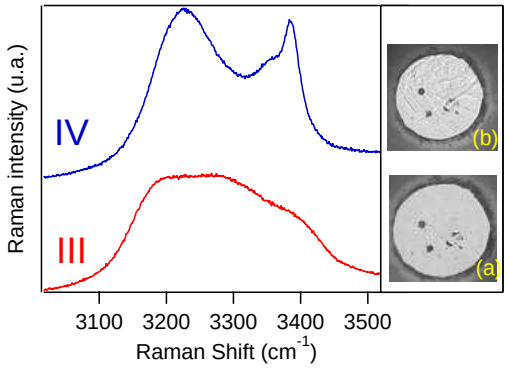

FIG. 2: Raman spectra of solid NH_3 phases IV and III in the ν_1-ν_3 region. The spectra were collected at 373 K, 9.7 and 9 GPa. Photographs of polycrystalline samples of phase III (a) and IV (b) are shown in inset.

A ruby ball was also used below 600 K. The uncertainties on pressure measurements are typically less than 0.02 GPa at ambient temperature and around 0.15 GPa at 900 K.

Membrane diamond anvil cells (mDAC) made of high-temperature Inconel alloy were used. With a commercial ring-shaped resistive heater around the mDAC, sample temperatures up to 750 K could be obtained. Above 750 K, an internal heater located around the diamond-gasket assembly is used in addition. These heaters are temperature regulated within 1 K. During heating, a continuous flow of Ar/H_2 reducing gas mixture is directed onto the mDAC. The temperature of the sample was determined thanks to a K-type thermocouple fixed by ceramic cement on the head of one diamond, and cross-checked with the temperature determined *in situ* from the ruby up to 600 K[24]. With these techniques, a temperature uncertainty inferior to 5 K is obtained, as validated by previous studies[25,26,27].

Measurements of Raman spectra were performed using a T64000 spectrometer in backscattering geometry. Angular-dispersive x-ray diffraction spectra were collected on the ID09 station of the ESRF (Grenoble, France).

III. RESULTS AND DISCUSSION

A. III-IV transition line

The transition between the disordered phase III and ordered phase IV has been investigated as a function of pressure and temperature up to 20 GPa and 500 K. The transition

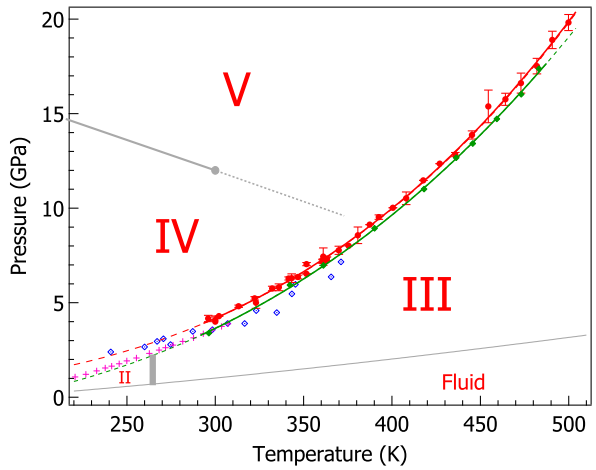

FIG. 3: The III-IV transition line. Our experimental points in compression (dots) and decompression (green lozenge) are presented along with literature data (crosses: Kume *et al.*[17], diamonds: Hanson *et al.*[9]). Solid lines represent the fits to Simon-Glatzel equations (Eqs. [1,2,3])

pressure has been determined along isotherms during compression and decompression. We used several criteria to detect the transition: (1) by detecting the pressure discontinuity: a rapid pressure drop of a few tenth of GPa is observed at the III-IV transition due to the volume discontinuity (1.5% at 300 K[20]). The transition pressure is defined as the lower pressure; (2) by X-ray diffraction: patterns of phase III (cubic) and phase IV (orthorhombic) are easily recognizable; (3) by visual observation: reticulation is observed in phase IV (birefringent phase), which disappears in phase III (see pictures in Fig. 2); (4) by Raman spectroscopy: the shape of the $\nu_1 - \nu_3$ band is very different between the two phases; the modes are broad in the disordered phase III and sharper in the ordered phase IV (Fig. 2).

Our experimental points are presented in Fig. 3 and in Table I. They form two distinct transition curves corresponding respectively to compression and decompression measurements. These two data sets are well fitted by the following Simon-Glatzel (SG) type equations[28] :

$$P_{III\rightarrow IV}(T) = 3.9(1) + 3.7(2)\left[\left(\frac{T}{293.15}\right)^{3.1(1)} - 1\right] \quad (1)$$

$$P_{IV\rightarrow III}(T) = 3.3(1) + 4.5(4)\left[\left(\frac{T}{293.15}\right)^{2.8(1)} - 1\right] \quad (2)$$

Taking the average of these two curves as the transition line gives the following SG

equation:

$$P_{IV \rightleftarrows III}(T) = 3.6(2) + 4.1(6) \left[\left(\frac{T}{293.15} \right)^{3.0(2)} - 1 \right] \quad (3)$$

The use of the SG equation is usually restricted to the description of melting curves. We note though that this phenomenological law is valid for any first-order phase transition satisfying Clausius-Clapeyron's relation ($dP/dT = \Delta H/T\Delta V$ where ΔH and ΔV are the enthalpy and volume discontinuities at the transition), provided that $\Delta H/\Delta V$ is a linear function of pressure[29]. The III-IV transition is a first-order transition between a plastic phase (III) where the H atoms are highly disordered (they may occupy as much as 192 positions[30]) and an ordered phase (IV) where H atoms have definite positions. The fcc packing in phase III also indicates the weak influence of the H-bonds in this phase. This phase transition can thus be viewed as a pseudo-melting of the hydrogen sublattice.

The experimental data points of Hanson and Jordan[9] and Kume *et al.*[17] are also presented in figure 3. Hanson and Jordan's transition pressures above 300 K are on average lower than ours but the slopes are very similar. A good agreement can also be observed between Kume *et al.*'s data and our experimental points taken on decompression.

Our main goal in studying the III-IV transition line was to detect whether the presence of the transition between the two isostructural solids IV and V detected at 12 GPa at 300 K had a measurable inference on this line, such as a discontinuity of slope. This is actually not the case, no discontinuity being observable within the precision of our measurements up to 500 K and 20 GPa. In our single-crystal x-ray diffraction experiments, the IV-V transition was detected thanks to the systematic and sudden splitting of the crystal and the discontinuous change of slope of the c/a ratio[20]. Although no volume jump could be measured within uncertainties ($\sim$ 0.06 cm^3/mol), the transition must be first-order since the two phases are isosymmetric. Using Raman spectroscopy, we observed a small jump in some lattice modes at 12 GPa, 300 K and around 20 GPa at 50 K[21]. In figure 3, the IV-V transition line based on these two points is drawn. The absence of discontinuity at the expected III-IV-V triple point (ca. 9 GPa, 390 K) is not really surprising since the volume difference between IV and V is very small. It is also possible that, between 300 and 380 K, the IV-V transition line ends at a critical point where the transition becomes second-order. The existence of such critical points have been predicted by Landau[31,32] and observed in a few materials such as Cr-doped V_2O_3[33], NH_4PF_6[34] and cerium[35]. The proximity of a Landau

TABLE I: Experimental data for the III-IV transition line. T is the temperature measured with the thermocouple in K. P is the pressure measured with the borate or the ruby in GPa.

$P_{III\rightarrow IV}$	$T_{III\rightarrow IV}$	$P_{III\rightarrow IV}$	$T_{III\rightarrow IV}$	$P_{III\rightarrow IV}$	$T_{III\rightarrow IV}$
3.69	291.0	7.33	363.0	13.90	445.3
4.00	298.0	7.47	361.1	14.92	454.5
4.08	298.0	7.66	369.9	15.41	454.5
4.16	298.0	7.80	369.9	15.78	464.2
4.29	302.1	8.00	375.5	16.64	473.0
4.52	313.5	8.04	375.5	16.71	473.0
4.81	313.2	8.59	380.6	17.54	482.0
5.03	323.0	9.05	384.4	18.92	490.7
5.06	323.0	9.16	387.4	19.84	499.9
5.23	322.3	7.33	363.0		
5.75	332.2	7.47	361.1		
5.79	336.0	7.66	369.9		
5.84	336.0	7.80	369.9		
5.93	328.8	8.00	375.5		
6.24	343.2	8.04	375.5		
6.28	341.5	8.59	380.6	$P_{IV\rightarrow III}$	$T_{IV\rightarrow III}$
6.32	343.2	9.05	384.4	17.37	483.1
6.55	351.6	9.16	387.4	16.02	473.1
6.58	351.6	9.55	392.5	14.72	459.3
6.36	346.6	9.89	400.5	13.42	445.7
7.04	351.6	10.05	400.5	12.66	436.3
7.18	360.5	10.39	408.0	11.00	418.1
7.22	360.9	10.55	408.0	8.95	390.1
7.24	361.1	11.50	417.7	6.97	361.1
7.26	361.9	12.21	427.0	5.93	342.2
7.31	362.7	12.68	435.8	3.39	296.3
7.31	361.1	12.86	435.8		

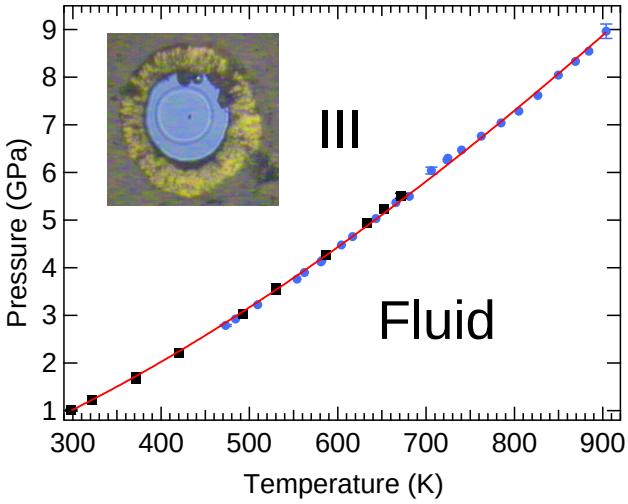

FIG. 4: Experimental melting points determined in this work. The symbols are associated with two separates experiments. The solid line represents the fit to our data with a Simon-Glatzel equation. The inset shows a photograph of the solid-fluid equilibrium at 473 K. A ruby ball and some samarium powder are visible.

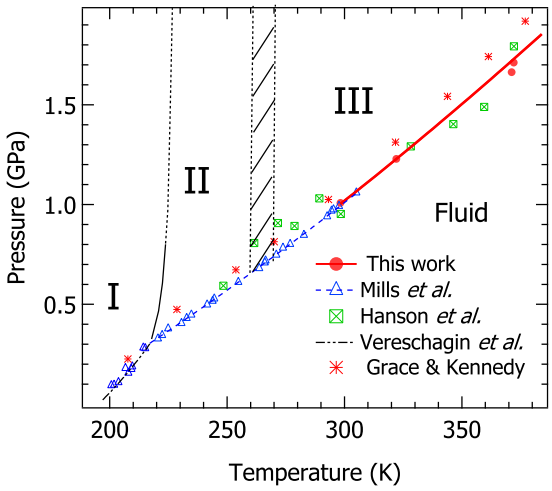

FIG. 5: Comparison of the melting line obtained in this work (red dots and line) with previous experimental studies[9,16,36,37].

critical point could also explain the weak volume discontinuity at ambient temperature.

B. The melting line

The melting curve was determined by visual observation of the solid-fluid equilibrium. This is possible because of the difference in refractive index between the fluid and solid phases which remains large enough to clearly distinguish the two phases up to 900 K (see inset of Fig. 4). The measurement of the sample pressure and temperature when this coexistence has been stabilized defines a melting point. The coexistence was kept during the slow heating of the sample by increasing the load. This method allows to precisely determine the melting curve and prevents problems associated with metastabilities such as undercooling or overpressurization.

Two different samples have been studied to determine the melting curve of NH_3 in the range [300-904 K] and [1-9 GPa]. The two measurements agree very well in the overlapping region (470-670 K). The experimental melting points are plotted in Fig. 4 (reported in table II) and compared to other melting studies[9,16,36,37] in Fig. 5. Our data agree with previous measurements from Hanson and Jordan[9] up to 373 K within their stated uncertainty of 0.1 GPa. The melting pressures determined by Grace and Kennedy[37] in a piston-cylinder apparatus are systematically higher than ours and those of Mills *et al.*[16] by 0.08–0.13 GPa. In the P-T range covered by our experiments, the melting pressure is a monotonous increasing function of temperature and no discontinuity is observed. The whole data set is well fitted by the following Simon-Glatzel equation[43]:

$$P(T) = 0.307 + 1.135(51)\left[\left(\frac{T}{217.34}\right)^{1.510(31)} - 1\right] \quad (4)$$

In the latter expression, we used as reference P-T point the I-II-fluid triple point coordinates of NH_3 (P=0.307 GPa and T=217.34 K)[16]. As a matter of fact, the II-III-fluid triple point has not been determined yet: no discontinuity has been observed on the melting curve[16] at the expected location for this triple point (around 265 K[38]). Phase II differs from phase III by its hexagonal compact ordering of the molecules, but both are plastic phases with large orientational disorder. The absence of discontinuity observable on the melting curve at the triple point indicates that the two phases have very similar free energies. The extrapolation of our melting curve down to the I-II-triple point reproduces very well the melting data of Mills *et al.*[16]. Actually, the parameters of the Simon-Glatzel form in Eq. 4, obtained by fitting our data alone, are identical within standard deviations to those

TABLE II: Experimental data for the melting line. T_m is the temperature measured with the thermocouple in K. P_m is the pressure measured with the borate in GPa.

P_m	T_m	P_m	T_m
1.01	298.3	4.94	6 33.0
1.23	322.0	5.03	6 43.1
1.66	371.1	5.24	6 52.9
1.71	372.0	5.37	6 65.8
2.21	420.1	5.50	681.1
2.79	473.1	5.51	671.7
2.93	484.3	6.04	705.9
3.03	492.8	6.26	723.4
3.22	509.4	6.30	724.6
3.53	529.9	6.47	740.1
3.57	530.4	6.76	762.6
3.76	553.8	7.04	784.5
3.90	562.1	7.29	805.1
4.12	580.8	7.62	826.4
4.15	582.0	8.04	849.6
4.26	586.3	8.33	869.0
4.48	604.1	8.55	884.3
4.65	616.8	8.97	903.9

determined by Mills *et al.*[16] by fitting their own melting data between 220.5 and 305 K.

The melting line of NH_3 is compared to those of the isoelectronic solids H_2O[25], CH_4[44] and neon[26,39] in Fig. 6. This comparison is shown both on a absolute P-T scale and using reduced units[45] to rescale the melting lines on the same density map. Although none of these solids "corresponds" *stricto sensu*, it can be seen that the melting line of NH_3 is closer to that of methane than to the one of water at high P-T. In particular, the slopes dT_m/dP_m of the melting curves of NH_3 and CH_4 are very similar and much less pressure dependent than for H_2O. Since the main difference between CH_4 and H_2O, in terms of intermolecular

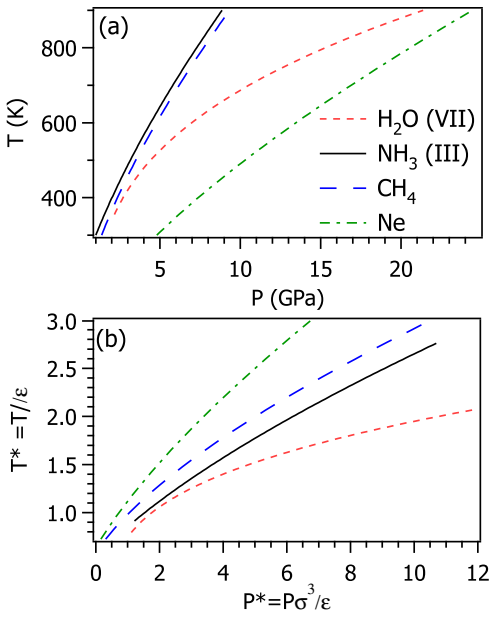

FIG. 6: (Color online) Comparison between the melting lines of the isoelectronic solids H_2O, NH_3, CH_4 and Ne on absolute (a) and reduced (b) scales.

interactions, is the absence of hydrogen bonds in CH_4, the similitude between CH_4 and NH_3 indicates that the hydrogen bonds have little influence on the melting properties of NH_3 in the P-T range covered by our experiments.

C. Phase diagram at high temperatures: comparison with *ab initio* calculations

To compare our experimental results to the *ab initio* molecular dynamics (AIMD) simulation of Cavazzoni *et al.*[3], we reproduced the phase diagram predicted by these authors in Fig. 7. Since the calculations probed pressures above 30 GPa, comparison can only be made with the extrapolation of the Simon-Glatzel equations determined for both the III-IV phase line (Eq. [3]) and the melting line (Eq. [4]). Starting from a sample of phase IV at 30 GPa, Cavazzoni *et al.* observed a phase transition to a hcp plastic phase at ca. 500 K and then melting around 1500 K. At 60 GPa, the ordered-plastic phase transition was observed between 500 and 1000 K, succeeded by the plastic-superionic phase transition between 1000 K and 1200 K. This superionic phase was also obtained at 150 and 300 GPa in the same temperature range. Although phase III is fcc, we have observed above that the difference in free energy between the hcp and fcc plastic phases is very small, so we can assimilate the hcp

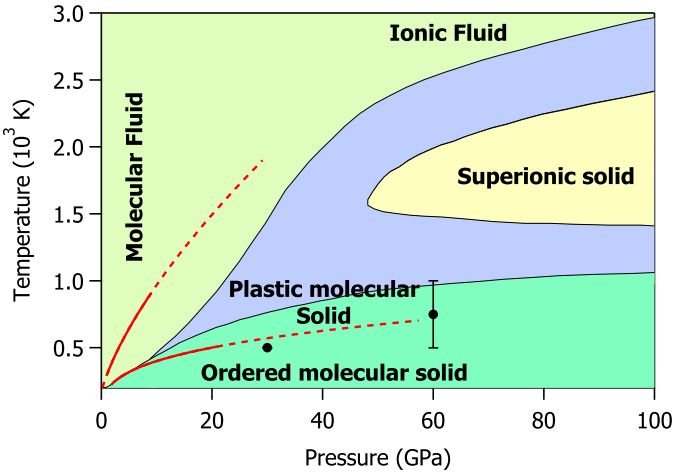

FIG. 7: (Color online) Phase diagram of ammonia according to *ab initio* molecular dynamics simulations of Ref. 3. Fits to present experimental data (red solid lines) and their extrapolations (broken lines) are shown. The black dots represent P-T points where simulations predict a transition between phase IV and a hcp plastic solid.

plastic phase obtained by Cavazzoni *et al.* with phase III. The extrapolation of our III-IV transition line puts the transition at 570 K at 30 GPa and 720 K at 60 GPa, i.e. close to the predicted ones. On the other hand, the experimental and calculated melting lines are rather different. Cavazzoni *et al.* predict a melting temperature of ∼1500 K at 30 GPa, that is 400 K lower than the extrapolation of our Simon-Glatzel fit. It is rather surprising since AIMD simulations usually tend to overestimate the melting temperature[40]. If we rely on calculations, a strong deviation from the behaviour predicted by the Simon-Glatzel equation should be observed between 9 and 30 GPa. This is one motivation to pursue the experiments to higher P-T conditions.

IV. CONCLUSIONS

In this paper, we have presented an experimental investigation of the high P-T phase diagram of NH_3. We have examined the evolution of the III-IV transition line up to 500 K and of the melting curve up to 900 K. These two first-order transition lines can be well fitted with Simon-Glatzel equations and no discontinuities have been observed on both lines. The presence of a Landau critical point ending the IV-V first-order transition line is a possible explanation for the non-observation of the III-IV-V triple point. A good agreement is found

between the extrapolation of present measurements and *ab initio* predictions of the ordered-plastic solid transitions, but not for the melting curve. Higher P-T conditions need to be probed to evidence the predicted superionic phase.

Acknowledgments

The authors are indebted to B. Canny for his help in preparing the experiments and acknowledge the ESRF for provision of beamtime.

---

* Electronic address: sandra.ninet@impmc.jussieu.fr

[1] W. B. Hubbard, Science **214**, 145 (1981).

[2] W. Hubbard, M. Podoloak, and D. Stevenson, *Neptune and Triton* (D.P. Cruikshank, 1995).

[3] C. Cavazzoni, G. Chiarotti, S. Scandolo, E. Tosatti, M. Bernasconi, and M. Parrinello, Science **283**, 44 (1999).

[4] N. Goldman, L. E. Fried, I.-F. W. Kuo, and C. J. Mundy, Phys. Rev. Lett. **94**, 217801 (2005).

[5] A. F. Goncharov, N. Goldman, L. E. Fried, J. C. Crowhurst, I. F. W. Kuo, C. J. Mundy, and J. M. Zaug, Phys. Rev. Lett. **94**, 125508 (2005).

[6] B. Schwager, L. Chudinovskikh, A. Gavriliuk, and R. Boehler, J. Phys.: Condens. Matter **16**, 1177 (2004).

[7] J.-F. Lin, E. Gregoryanz, V. V. Struzhkin, M. Somoayazulu, H.-K. Mao, and R. J. Hemley, Geophys. Res. Lett. **32**, L11306 (2005).

[8] N. A. Dubrovinskaya and L. Dubrovinsky, in *Annual report of the Bayerisches Geoinstitut* (2004), p. 34, URL `http://www.bgi.uni-bayreuth.de/annual_report/2004/c_34.phtml`.

[9] R. C. Hanson and M. Jordan, J. Phys. Chem **84**, 1173 (1980).

[10] R. Dick, J. Chem. Phys **74**, 4053 (1981).

[11] A. Mitchell and W. J. Nellis, J. Chem. Phys **76**, 6273 (1982).

[12] W. J. Nellis, D. C. Hamilton, N. C. Holmes, H. B. Radousky, F. H. Ree, A. C. Mitchell, and M. Nicol, Science **240**, 779 (1988).

[13] H. Radousky, A. Mitchell, and W. Nellis, J. Chem. Phys **93**, 8235 (1990).

[14] W. J. Nellis, N. C. Holmes, A. C. Mitchell, D. C. Hamilton, and M. Nicol, J. Chem. Phys. **107**, 9096 (1997).

[15] J. S. Loveday, R. J. Nelmes, W. G. Marshall, J. M. Besson, S. Klotz, and G. Hamel, Phys. Rev. Lett. **76**, 74 (1996).

[16] R. L. Mills, D. H. Liebenberg, and P. Pruzan, J. Phys. Chem. **86**, 5219 (1982).

[17] T. Kume, S. Sasaki, and H. Shimizu, J. Raman Spectrosc. **32**, 383 (2001).

[18] M. Gauthier, P. Pruzan, J. C. Chervin, and J. M. Besson, Phys. Rev. B **37**, 2102 (1988).

[19] M. Gauthier, P. Pruzan, J. C. Chervin, and A. Polian, Solid State Comm. **68**, 149 (1988).

[20] F. Datchi, S. Ninet, M. Gauthier, A. M. Saitta, B. Canny, and F. Decremps, Phys. Rev. B **73**, 174111 (2006).

[21] S. Ninet, F. Datchi, and A. M. Saitta, to be published.

[22] S. Ninet, F. Datchi, A. M. Saitta, M. Lazzeri, and B. Canny, Phys. Rev. B **74**, 104101 (2006).

[23] F. Datchi, R. LeToullec, and P. Loubeyre, J. Appl. Phys. **81**, 3333 (1997).

[24] F. Datchi, A. Dewaele, Y. L. Godec, and P. Loubeyre, Phys. Rev. B **75**, 214104 (2007).

[25] F. Datchi, P. Loubeyre, and R. LeToullec, Phys. Rev. B **61**, 6535 (2000).

[26] F. Datchi and B. Canny, Phys. Rev. B **69**, 144106 (2004).

[27] V. M. Giordano and F. Datchi, Europhys. Lett. **77**, 46002 (2007).

[28] F. Simon and G. Glatzel, Z. Annorg. Allg. Chem. **178**, 309 (1929).

[29] A. V. Voronel, Sov. Phys. Tech. Phys. **3**, 2458 (1958).

[30] R. B. VonDreele and R. C. Hanson, Acta Cryst. **C40**, 1635 (1984).

[31] J. C. Tolédano and P. Tolédano, *The Landau theory of phase transitions* (World Scientific, 1987).

[32] L. Landau and E. Lifchitz, *Statistical physics* (Ellipses, 1967).

[33] A. Jayaraman, D. B. McWhan, J. P. Remeika, and P. D. Dernier, Phys. Rev. B **2**, 3751 (1970).

[34] I. P. Swainson, R. P. Hammond, J. K. Cockcroft, and R. D. Weir, Phys. Rev. B **66**, 174109 (2002).

[35] R. I. Beecroft and C. A. Swenson, J. Phys. Chem. Solids **15**, 234 (1960).

[36] L. F. Vereschagin and F. F. Voronov, Z. Fizi. Khimi. **30**, 329 (1958).

[37] J. D. Grace and G. C. Kennedy, J. Phys. Chem. Solids **28**, 977 (1967).

[38] R. L. Mills and B. Olinger, unpublished.

[39] W. L. Vos, J. A. Schouten, D. A. Young, and M. Ross, J. Chem. Phys. **94**, 3835 (1991).

[40] L. Koci, R. Ahuja, and A. B. Belonoshko, Phys. Rev. B **75**, 214108 (2007).

[41] U. Setzmann and W. Wagner, J. Phys. Chem. Ref. Data **20**, 1061 (1991).

[42] A. Belonoshko and S. K. Saxena, Geochim. Cosmochim. Acta **56**, 3611 (1992).

[43] Numbers in parentheses indicate the 95% confidence interval for the fit parameters

[44] The melting line of methane has only been determined up to 400 K. At higher temperatures, we use the extrapolation of the melting law given in Ref. 41

[45] We use reduced units derived from the law of corresponding states : $P^* = P\sigma^3/\epsilon$, $T^* = T/\epsilon$, where σ and ϵ are respectively the position and depth of the mimimum of the effective pair potential. For these two parameters, we use the values determined for the exp-6 potential by Belonoshko and Saxena[42] for H_2O, NH_3 and CH_4, and by Vos *et al.* [39] for Ne.